

ASTROD and ASTROD I: *Progress Report*

A. Pulido Patón

*Purple Mountain Observatory, Chinese
Academy of Sciences, Nanjing 210008*

**GWADW 2006,
Isola d'Elba, May 27-June 2nd**

LIGO-G060325-00-Z

The road towards ASTROD

- Laser Astrodynamics is proposed to study relativistic gravity and to explore the solar system, 2nd William Fairbank conference (Hong Kong), and International workshop on Gravitation and Fifth Force (Seoul) 1993.
- A multi-purpose astrodynamical mission is reached (1994) in 7th Marcel Grossmann, July, 1994, Stanford (California).
- **ASTROD (Astrodynamical Space Test of Relativity using Optical Devices)** presented at 31st COSPAR Scientific Assembly July 1996.
- ASTROD and its sensitivity to \dot{G} measurements presented in the Pacific conference on Gravitation and Cosmology. Seoul (Korea) February 1996.
- ASTROD and its related gravitational wave sensitivity presented at TAMA Gravitational Wave Workshop in Tokyo (Japan) 1997.
- The possibility of solar g-mode detection was presented in 3rd Edoardo Amaldi and 1st ASTROD Symposium (2001).

Current Collaborators

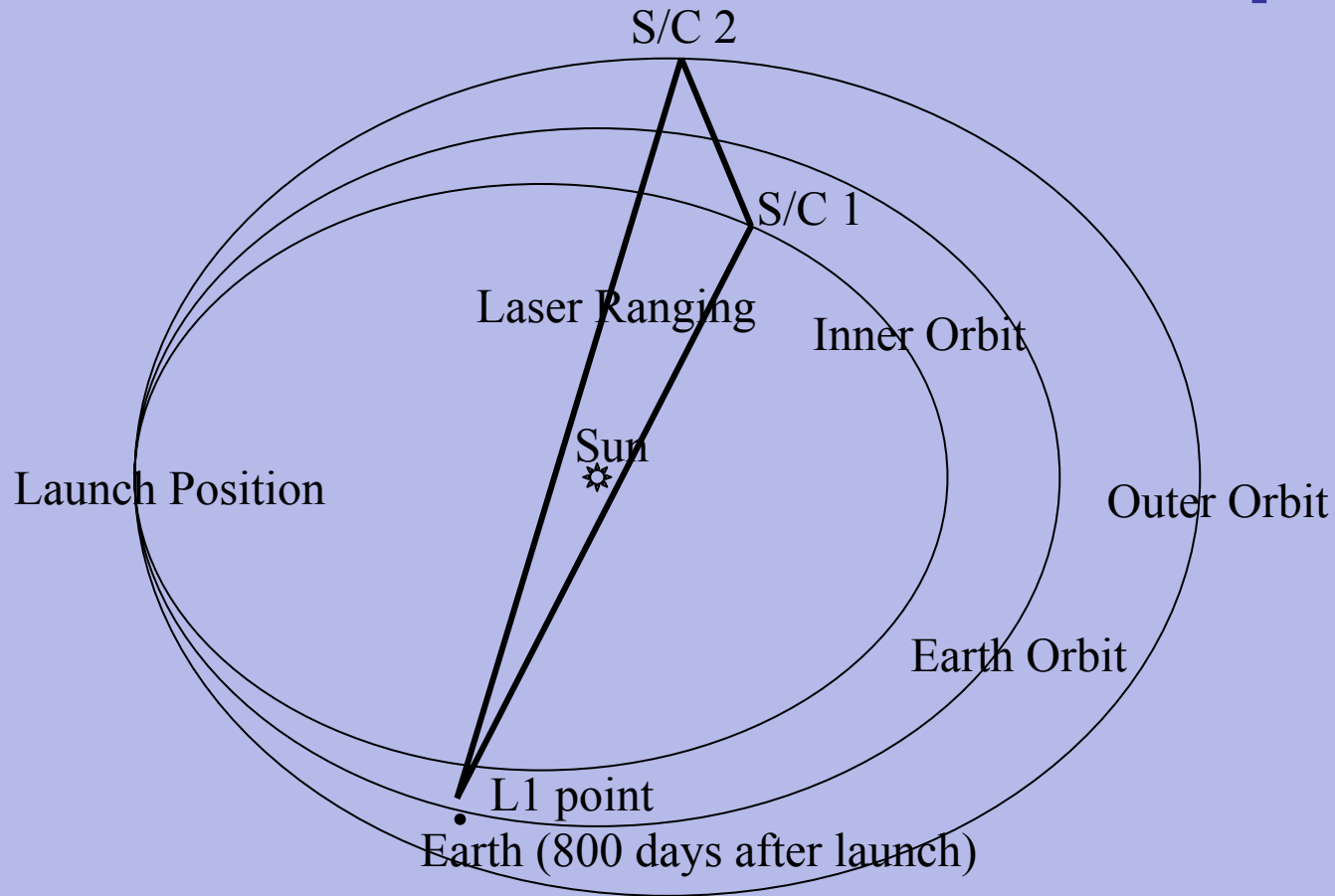
**Wei-Tou Ni^{1,2,3}, Henrique Araújo⁴, Gang Bao¹, Hansjörg Dittus⁵,
Tianyi Huang⁶, Sergei Klioner⁷, Sergei Kopeikin⁸, George
Krasinsky⁹, Claus Lämmerzahl⁵, Guangyu Li^{1,2}, Hongying Li¹,
Lei Liu¹, Yu-Xin Nie¹⁰, Antonio Pulido Patón¹, Achim Peters¹¹,
Elena Pitjeva⁹, Albrecht Rüdiger¹², Étienne Samain¹³, Diana
Shaul⁴, Stephan Schiller¹⁴, Sachie Shiomi³, M. H. Soffel⁷,
Timothy Sumner⁴, Stephan Theil⁵, Pierre Touboul¹⁵, Patrick
Vrancken¹³, Feng Wang¹, Haitao Wang¹⁶, Zhiyi Wei¹⁰, Andreas
Wicht¹⁴, Xue-Jun Wu^{1,17}, Yan Xia¹, Yaoheng Xiong¹⁸, Chongming
Xu^{1,17}, Dong Peng⁶, Xie Yi⁶, Jun Yan^{1,2}, Hsien-Chi Yeh¹⁹, Yuan-
Zhong Zhang²⁰, Cheng Zhao¹, and Ze-Bing Zhou²¹**

- 1 Center for Gravitation and Cosmology, Purple Mountain Observatory, Chinese Academy of Sciences, Nanjing, 210008 China
- 2 National Astronomical Observatories, CAS, Beijing, 100012 China
- 3 Center for Gravitation and Cosmology, Department of Physics, Tsing Hua University, Hsinchu, Taiwan 30013
- 4 Department of Physics, Imperial College of Science, Technology and Medicine, London, SW7 2BW, UK
- 5 ZARM, University of Bremen, 28359 Bremen, Germany
- 6 Department of Astronomy, Nanjing University, Nanjing, 210093 China
- 7 Lohrmann-Observatorium, Institut für Planetare Geodäsie, Technische Universität Dresden, 01062 Dresden, Germany
- 8 Department of Physics and Astronomy, University of Missouri-Columbia, Columbia, Missouri 65221, USA
- 9 Institute of Applied Astronomy, Russian Academy of Sciences, St.-Petersburg, 191187 Russia
- 10 Institute of Physics, Chinese Academy of Sciences, Beijing, 100080 China
- 11 Department of Physics, Humboldt-University Berlin, 10117 Berlin, Germany
- 12 Max-Planck-Institut für Gravitationsphysik, 85748 Gärching, Germany
- 13 Observatoire de la Côte D'Azur, 06460 Caussols, France
- 14 Institute for Experimental Physics, University of Düsseldorf, 40225 Düsseldorf, Germany
- 15 Office National D'Études et de Recherches Aérospatiales, Chatillon Cedex, France
- 16 College of Automation Engineering, Nanjing University of Aeronautics and Astronautics, Nanjing, 210016 China
- 17 Department of Physics, Nanjing Normal University, Nanjing, 210097 China
- 18 Yunnan Observatory, NAOC, Chinese Academy of Sciences, Kunming, 650011 China
- 19 Division of Manufacturing Engineering, Nanyang Technological University, Singapore 639798
- 20 Institute of Theoretical Physics, CAS, Beijing, 100080 China
- 21 Department of Physics, Hua Zhong University of Science and Technology, Wuhan, 430074 China

International collaboration period

- 2000: ASTROD proposal submitted to ESA F2/F3 call (2000)
- 2001: 1st International ASTROD School and Symposium held in Beijing; Mini-ASTROD study began
- 2002: Mini-ASTROD (ASTROD I) workshop, Nanjing
- 2004: German proposal for a German-China ASTROD collaboration approved
- 2005: 2nd International ASTROD Symposium (June 2-3, Bremen, Germany)
- *2004-2005: ESA-China Space Workshops (1st & 2nd, Noordwijk & Shanghai), potential collaboration discussed*
- *2006(7): Joint ASTROD (ASTROD I) proposal to be submitted to ESA call for proposals*
- *2006: 3rd ASTROD Symposium (July 14-16, Beijing) before COSPAR (July 16-23) in Beijing*

ASTROD mission concept



ASTROD mission concept is to use three drag-free spacecraft. Two of the spacecraft are to be in an inner (outer) solar orbit employing laser interferometric ranging techniques with the spacecraft near the Earth-Sun L1 Lagrange point. Spacecraft payload: a proof mass, two telescopes, two 1 W lasers, a clock and a drag-free system.

ASTROD scientific objectives

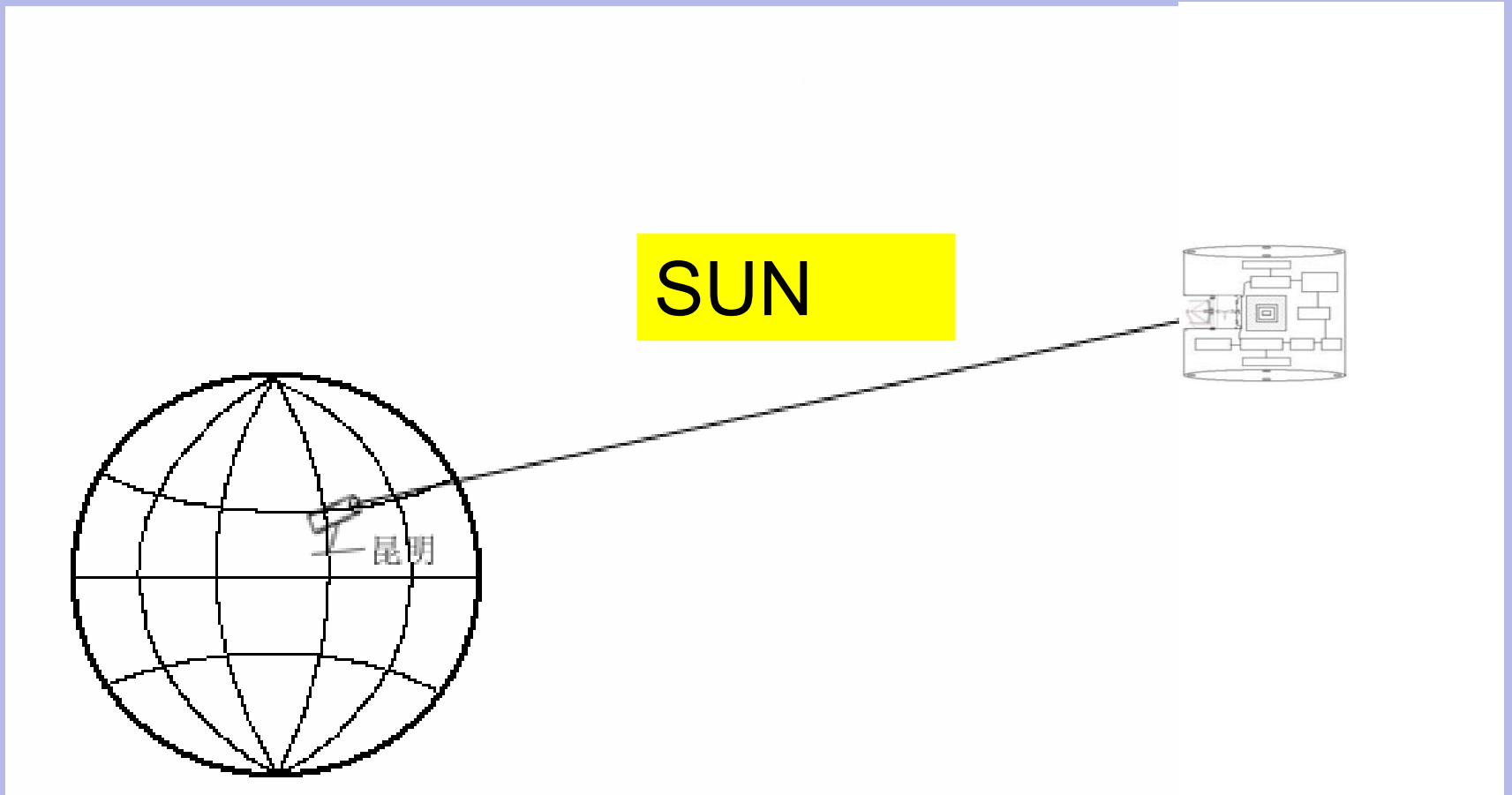
- Test Relativistic gravity with 3-5 orders of magnitude improvement in sensitivity. That includes the measurement of relativistic parameters β , γ , measurement of dG/dt , and the anomalous constant acceleration towards the Sun (Pioneer anomaly).
- Improvement by 3-4 orders of magnitude in the measurements of solar, planetary and asteroids parameters. That also includes a measurement of solar angular momentum via Lense-Thirring effect and the detection of solar g-modes by their changing gravity field.
- Detection of low frequency gravitational waves (5 μ Hz-5 mHz) from massive black hole and galactic binary stars. Background gravitational waves will also be explored.

ASTROD technological requirements

- Weak-light phase locking to 100 fW.
- Heterodyne interferometry and data analysis for unequal-arm interferometry.
- Coronagraph design and development: sunlight in the photodetectors should be less than 1 % of the laser light.
- High precision space clock and/or absolute stabilized laser to 10^{-17} .
- Drag-free system. Accelerometer noise requirement: $(0.3-1) \times 10^{-15} [1 + 10 \times (f/3\text{mHz})^2] \text{ ms}^{-2}\text{Hz}^{-1/2}$ at $0.1 \text{ mHz} < f < 100 \text{ mHz}$.
- Laser metrology to monitor position and distortion of spacecraft components for gravitational modeling.

ASTROD I

- ASTROD I is a simple version of ASTROD mission in which a single spacecraft in solar orbit and a ground laser station perform two-way interferometric and pulse laser ranging.



ASTROD orbit design features

- The distance to the Sun of the inner spacecraft varies from 0.77 AU to 1 AU and for the outer spacecraft varies from 1 AU to 1.32 AU.
- The two spacecraft should go to the other side of the sun simultaneously to perform Shapiro time delay.
- To obtain better accuracy in the measurements of \dot{G} and asteroid parameters' estimation, one spacecraft should be in inner orbit and the other in outer orbit.
- The two spacecraft at the other side of the sun should be near to each other for ranging in order to perform measurements of Lense-Thirring effect (measurement of solar angular momentum).

Relativistic parameter determination for ASTROD

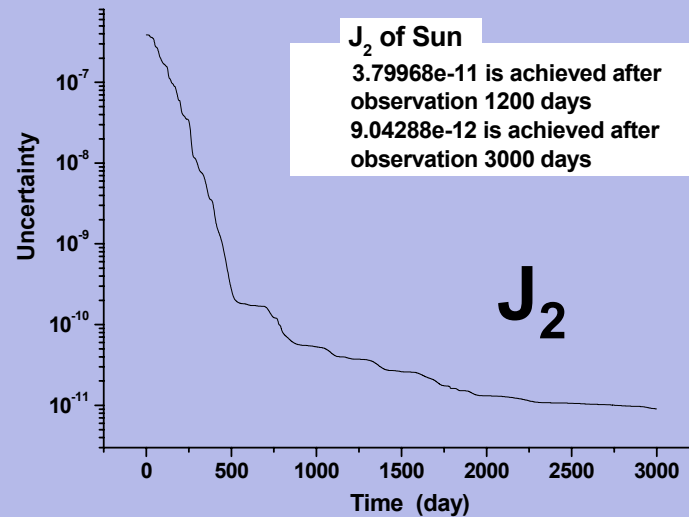
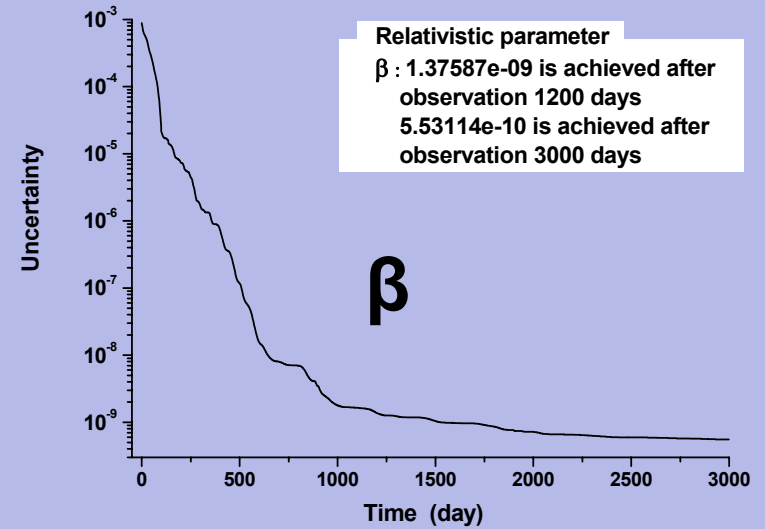
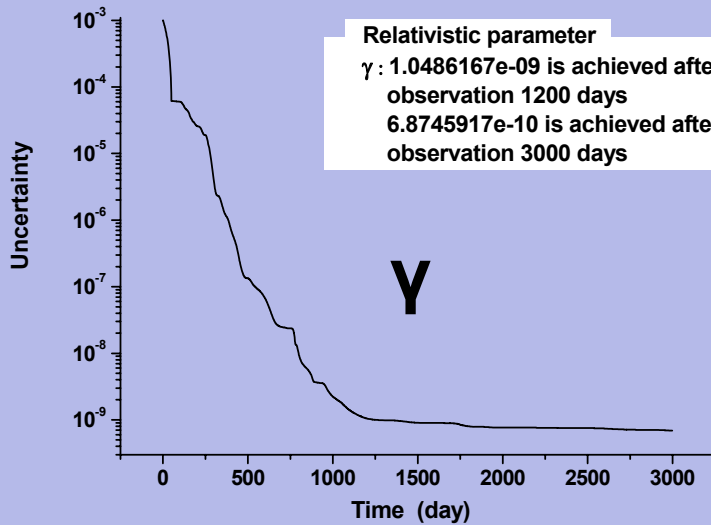
- The uncertainty of relativistic parameters (β, γ and J_2) assuming 1 ps accuracy and ASTROD acceleration noise $\sim 3 \times 10^{-18}$ m s $^{-2}$ (0.1 mHz) are, 1200 days after launch:

$$\gamma \approx 1.05 \times 10^{-9};$$

$$\beta \approx 1.38 \times 10^{-9} \text{ and}$$

$$J_2 \approx 3.8 \times 10^{-11}$$

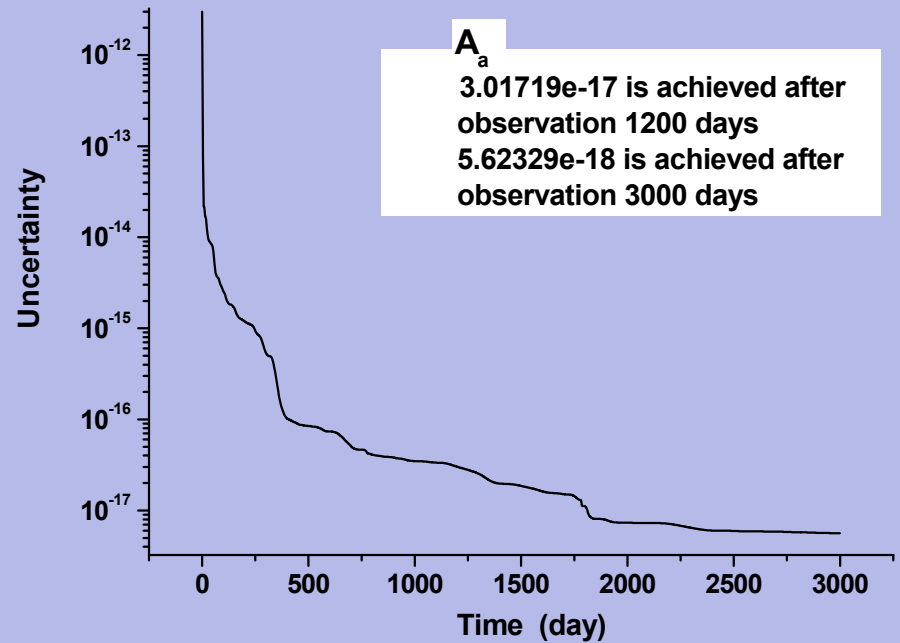
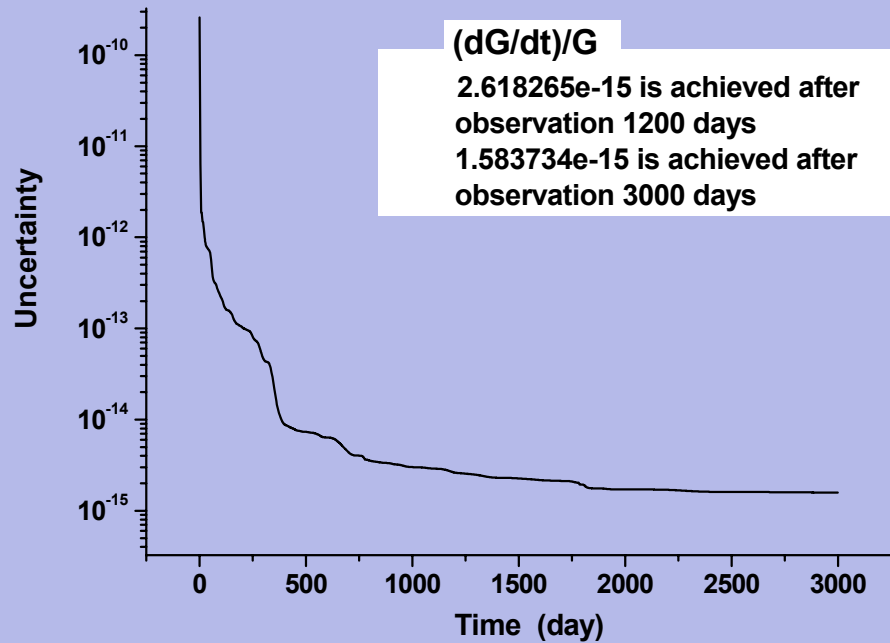
Relativistic parameter uncertainty evolution



Solar angular momentum

- Lense-Thirring effect can be measured by taking the time difference between the light round trips *SC1 - SC2 - Earth system basis* and *SC2 - SC1 - Earth System basis*.
- The Newtonian time difference t_1-t_2 for 800-1034 days after launching gives about 10 ms. The Lense-Thirring effect has a totally different signature and for this period of time is about 100 ps.
- Assuming a laser stability of 10^{-15} - 10^{-13} one could achieve 10^{-5} - 10^{-7} level of uncertainty.
- Lense-Thirring effect is proportional to the solar angular momentum.

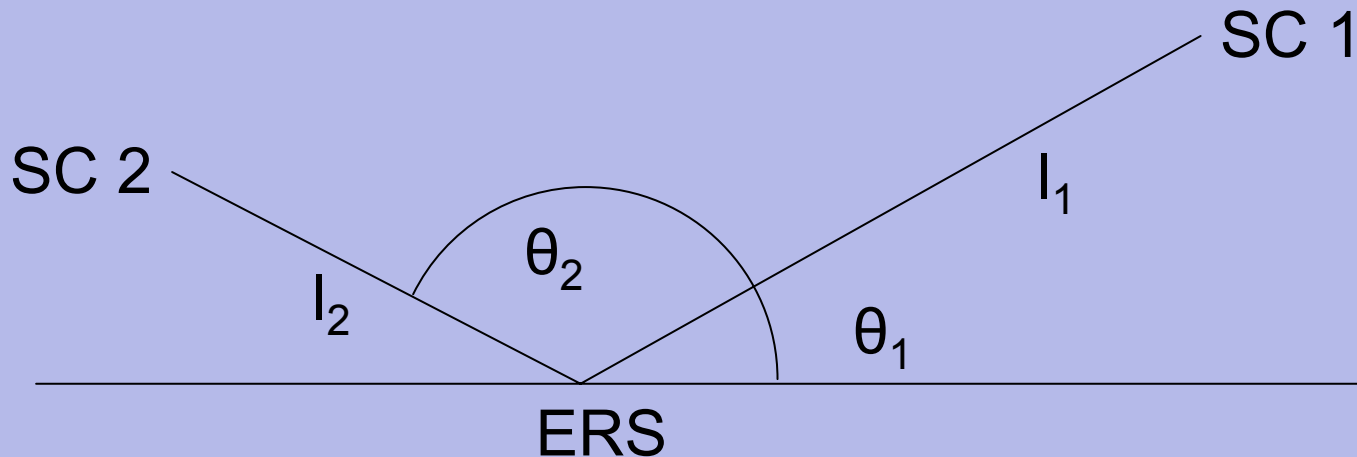
Evolution of \dot{G}/G and Pioneer anomaly uncertainties



\dot{G} measurement and anomalous acceleration towards the Sun

- $\dot{G}/G \approx 2.82 \times 10^{-15} \text{ yr}^{-1}$ and the anomalous acceleration towards the sun $A_a \approx 3.02 \times 10^{-17} \text{ m s}^{-2}$ (again assuming 1 ps and $3 \times 10^{-18} \text{ m s}^{-2}$).
- By using an independent measurement of \dot{G} ASTROD would be able to monitor the solar mass loss rate. The expected solar mass loss rate: a) electromagnetic radiation $\sim 7 \times 10^{-14} M_{\text{sun}}/\text{yr}$, b) solar wind $\sim 10^{-14} M_{\text{sun}}/\text{yr}$, c) solar neutrino $\sim 2 \times 10^{-15} M_{\text{sun}}/\text{yr}$ and d) solar axions $\sim 10^{-15} M_{\text{sun}}/\text{yr}$.

Gravitational wave detection



Gravitational detection topology. Path 1: ERS-SC1-ERS-SC2-ERS. Path 2: ERS-SC2-ERS-SC1-ERS. To minimize the arm-length difference.

For example if a monochromatic gravitational wave with + polarization arrives orthogonal to the plane formed by SC1, 2 and ERS, then the optical path difference for laser light traveling through path 1 and 2 and returning simultaneously at the same time t , is given by

$$\Delta l = 4h_+(c/f_G)(\cos 2\theta_1 + \cos 2\theta_2) [\cos 2\pi f_G(\tau_1 - \tau_2) + \cos 2\pi f_G(\tau_1 + \tau_2)] \cos 2\pi f(t + \phi_0)$$

With $\tau_1 = 2l_1/c$ and $\tau_2 = 2l_2/c$.

Solar g-modes

- When the spacecraft moves in solar orbit the amplitude and direction of the solar oscillation signals are deeply modulated in addition to the modulation due to spacecraft maneuvering.
- Time constants for solar oscillations are about 10^6 yr for low- l g-modes and over 2-3 months for low- l p-modes. Close white dwarf binaries (CWDB) time constant are longer than 10^6 yr. Hence confusion background is steady in inertial space, only modulated by spacecraft maneuvering and not by spacecraft orbit motion.
- With this extra modulation due to orbit motion the solar oscillation signals can reach 5 orders lower than the binary confusion limit.

Technological requirements: ASTROD (I) drag-free

ASTROD I acceleration noise of free fall test masses

$$\frac{S_{f_x}^{1/2}}{m} \approx 3 \times 10^{-14} \left[\left(\frac{0.3 \text{ mHz}}{f} \right) + 30 \left(\frac{f}{3 \text{ mHz}} \right)^2 \right] \text{ ms}^{-2} \text{ Hz}^{-1/2}$$
$$10^{-4} \text{ Hz} \leq f \leq 0.1 \text{ Hz}$$

LISA acceleration noise of free fall test masses

$$\frac{S_{f_x}^{1/2}}{m} \leq 3 \times 10^{-15} \left[1 + \left(\frac{f}{3 \text{ mHz}} \right)^2 \right] \text{ ms}^{-2} \text{ Hz}^{-1/2}$$
$$10^{-4} \text{ Hz} \leq f \leq 0.1 \text{ Hz}$$

ASTROD aims to improve LISA acceleration noise at **0.1 mHz** by a factor 3-10, i.e., approx. **$0.3\text{-}1 \times 10^{-15} \text{ ms}^{-2} \text{ Hz}^{-1/2}$** .

ASTROD bandwidth $5 \mu\text{Hz} \leq f \leq 5 \text{ mHz}$

ASTROD Gravitational Reference Sensor (GRS) preliminary concept

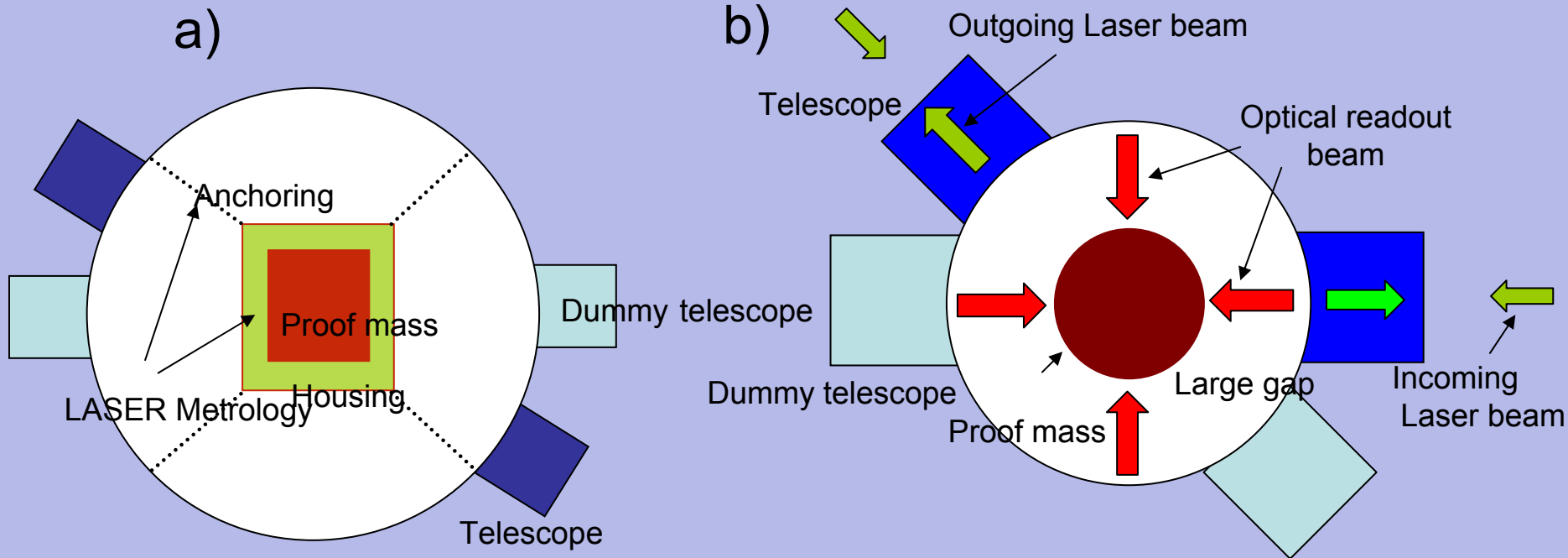
Move towards true drag-free conditions and **improving LISA drag-free performance by a factor 3-10.**

1. GRS provide reference positioning only. **Laser beam** does not **illuminate** directly the proof mass (avoiding cross coupling effects and pointing ahead problem) surface but **the GRS housing surface.**
2. Only **one** reference **proof mass.** GRS measures the center of mass position of the proof mass.
3. **Optical sensing** could replace capacitive sensing. Capacitance could still be used for control purposes.
4. Absolute laser metrology to measure structural changes due to thermal effects and slow relaxations.

LISA has adopted condition 1. Both conditions 1 and 2 avoid cross coupling due to control forces aimed to keep the right orientation of the proof mass mirror.

ASTROD will employ **separate interferometry** to measure the GW signal and the proof mass-spacecraft relative displacement independently.

ASTROD GRS

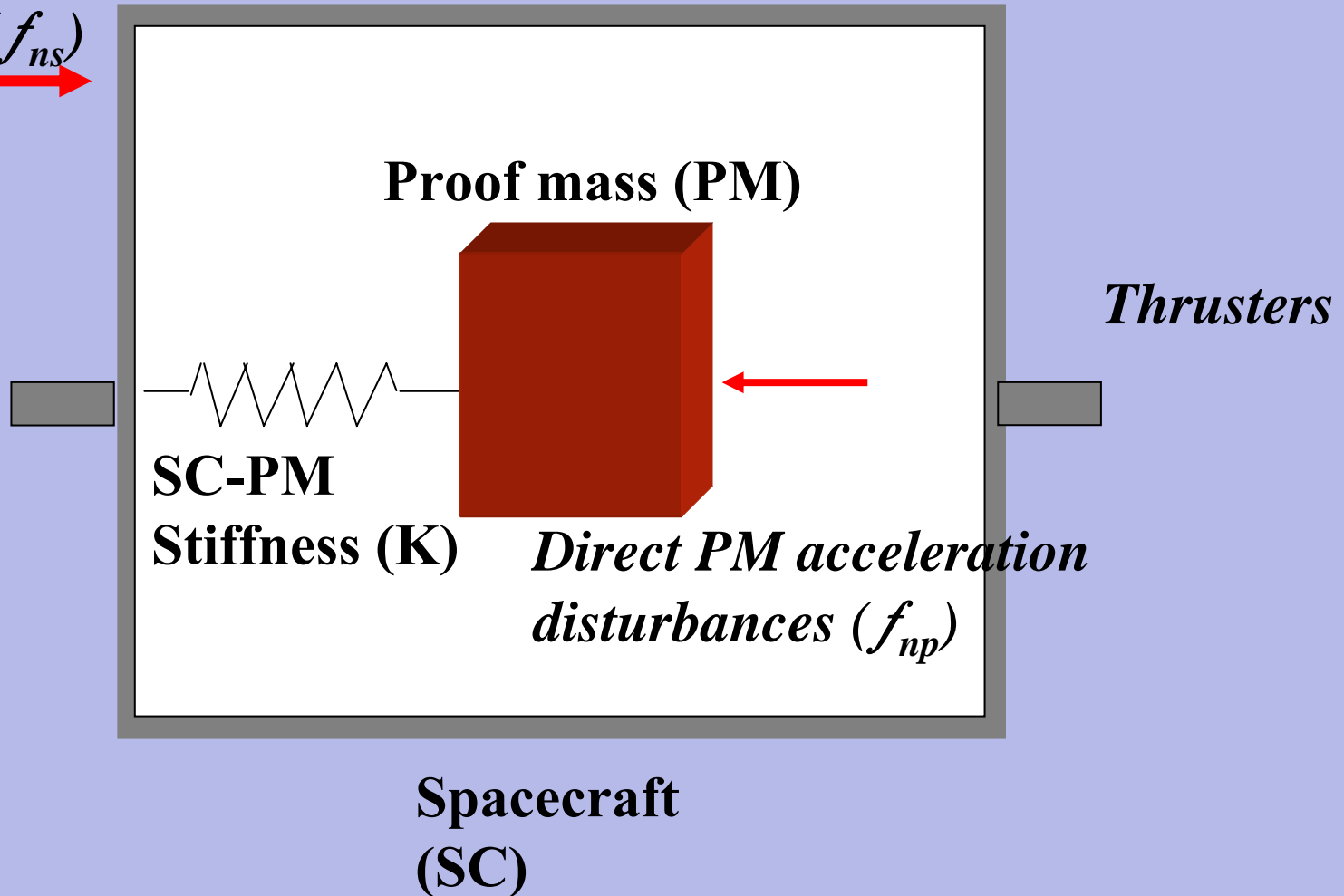


Schematic of possible GRS designs for ASTROD: a) a cubical proof mass free floating inside a housing anchored to the spacecraft, b) a spherical (cylindrical) proof mass is also considered.

Drag-free control concept

Spacecraft acceleration

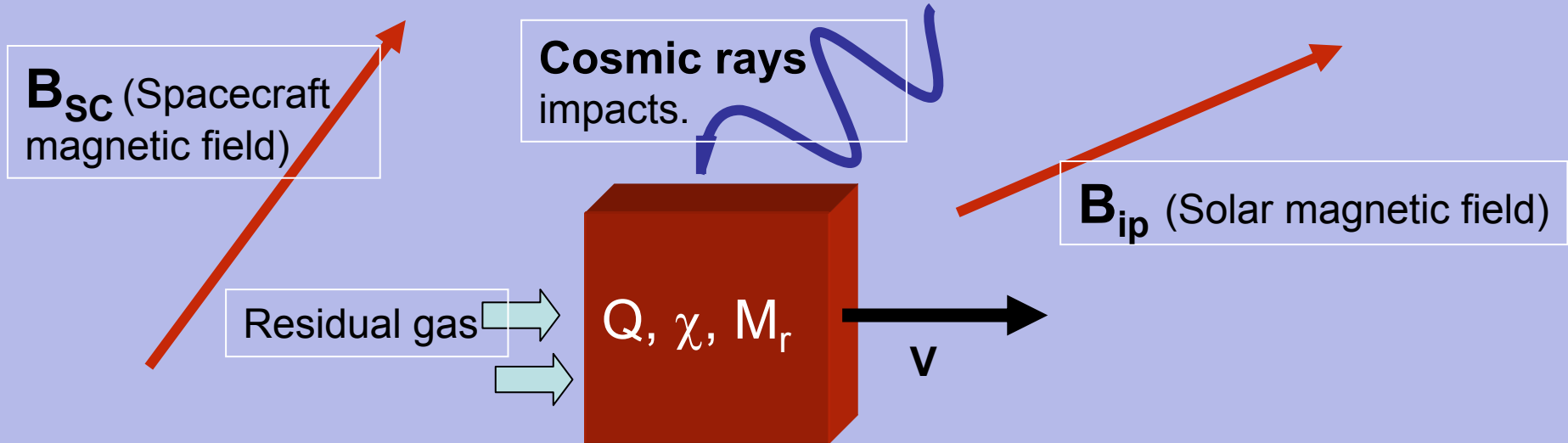
disturbances (f_{ns})



PM acceleration disturbance:

$$f_p \approx -\mathbf{K}\mathbf{X}_{nr} + f_{np} + (f_{ns} + \mathbf{T}\mathbf{N}_t)\mathbf{K}u^{-1}\omega^{-2}$$

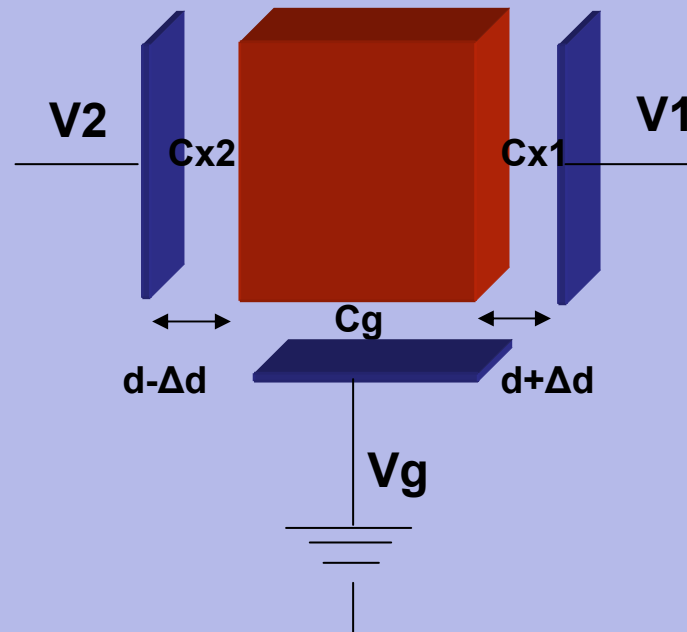
Direct proof mass acceleration disturbances



δT (temperature fluctuations) induces δP (pressure fluctuations) and **Gravity Gradients** in the spacecraft

- **Magnetic** interactions due to susceptibility (χ) and permanent moment of the proof mass (M_r)
- **Lorentz forces** due to proof mass charging (Q).
- **Thermal** disturbances (radiometer, out gassing, thermal radiation pressure and gravity gradients).
- **Impacts** due to cosmic rays and residual gas.

Capacitive sensing



- Capacitive sensing needs very close metallic surfaces to achieve good readout sensitivity.
- Displacement readout sensitivity is proportional to d^{-1} or d^{-2} for different readout configurations.
- By decreasing the gap, readout sensitivity increases but also back action disturbances and stiffness terms increase.

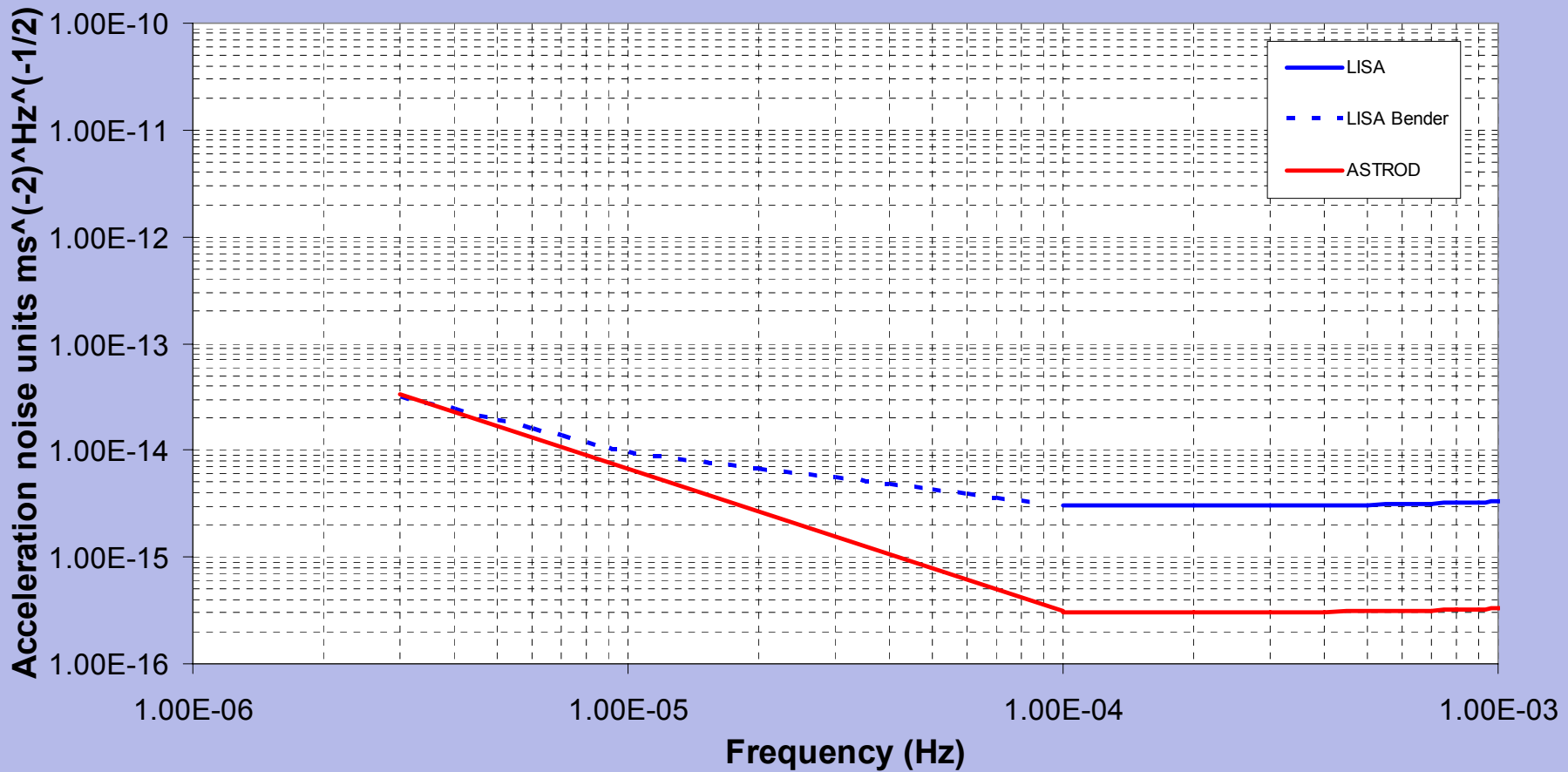
Optical sensing

- A drawback of capacitive sensing is the need for close gaps between metallic surfaces to increase sensitivity. The sensitivity is proportional to the difference between capacitance ($C_1 - C_2$), therefore proportional to d^{-2} .
- Optical sensing allows us using larger gaps between the PM and surrounding metallic surfaces.
- Optical sensing provides a way of sensing essentially free of stiffness.
- Optical sensing sensitivity is limited by shot noise. Picometer sensitivity can be achieved with μW of lasing power and $1.5 \mu\text{m}$ wavelength.

$$X_{nr} \approx \frac{1}{\pi} \left(\frac{hc\lambda}{2\eta P} \right)^{1/2}$$

- Back action force, $2P/c$, can be made negligible, with 1% compensation $\sim 10^{-17} \text{ m s}^{-2} \text{ Hz}^{-1/2}$.

LISA and ASTROD acceleration noise comparison



Detecting Gravitational Waves

- To estimate gravitational wave strength sensitivity

$$\sqrt{S_h^{M0}(f)} \approx \frac{1}{\sin cu_0} r_{SS} \left[\frac{4}{\pi^2} \left(\frac{hc}{\eta P_t} \right)^{1/2} \frac{\lambda^{3/2}}{D^2}, \frac{2A_0}{L(2\pi f)^2} \right] \text{Hz}^{-1/2}$$

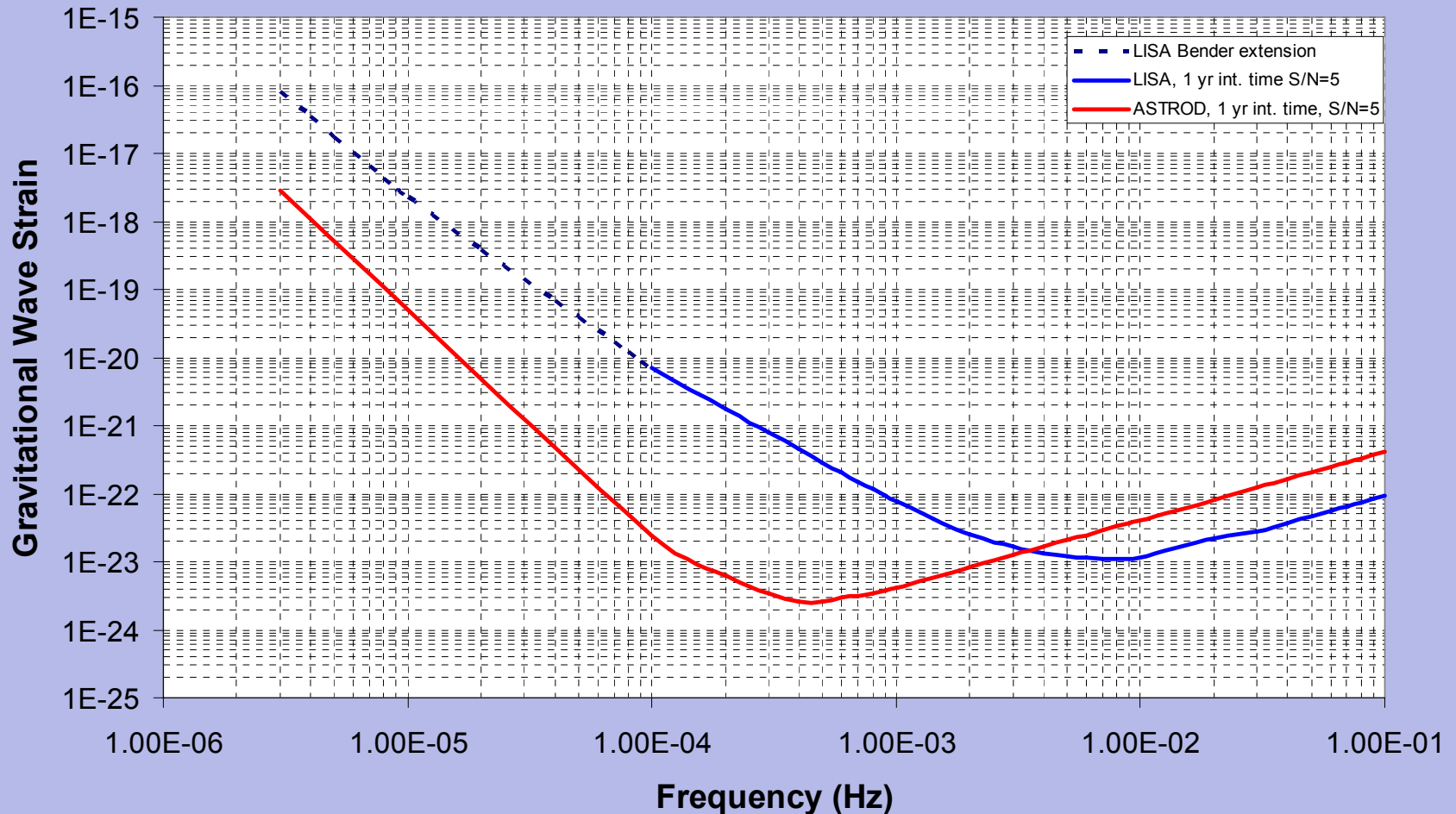
with $u_0 \equiv \frac{\omega L}{c}$

Lasing power (P_t): LISA **1W**, ASTROD **10 W**

Shot noise level (ASTROD) $\approx 1.2 \times 10^{-21}$

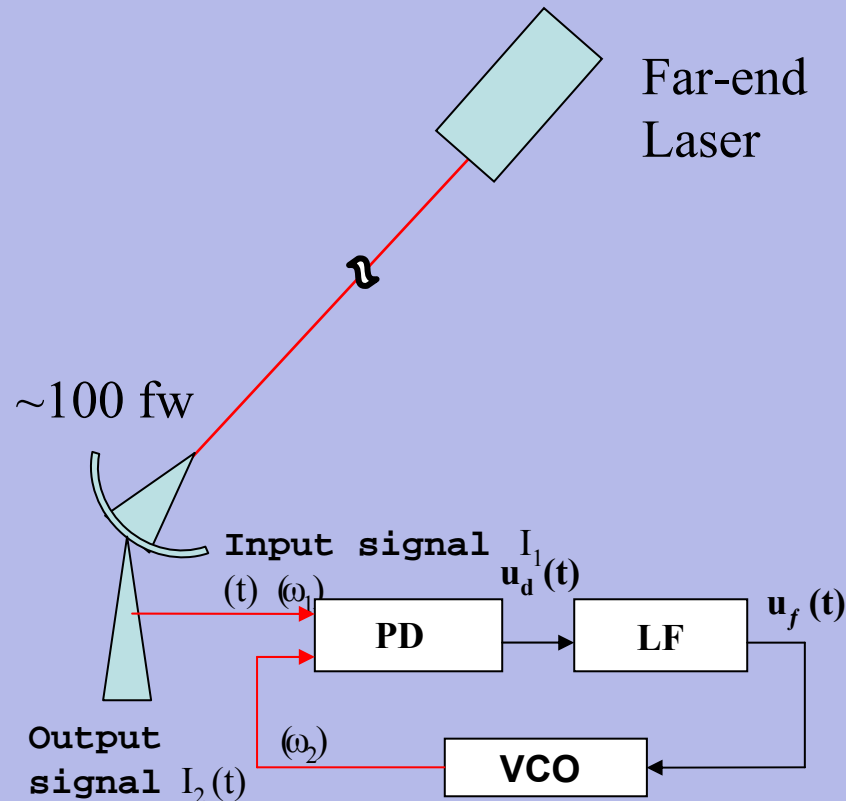
Acceleration noise (A_0) is the dominant source of noise at low frequencies.

LISA and ASTROD GW strain sensitivity ($S/N \approx 5$, int. time 1yr)



Picowatt and femtowatt weak light phase locking

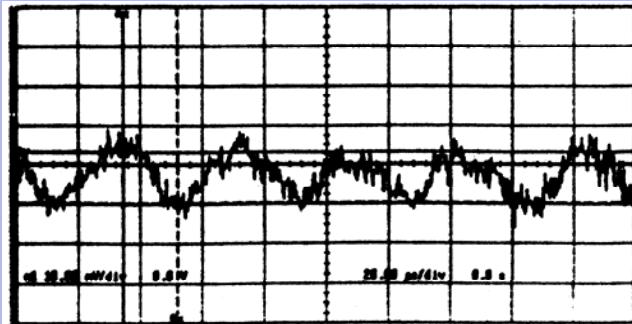
- **LISA** needs to achieve weak phase locking of the order of **85 pW**. Because of longer armlengths **ASTROD I** and **ASTROD** have to probe weak phase locking of the order of **100 femtowatts** (assuming 1 W lasing power from far spacecraft).



Laboratory research on weak light phase locking for ASTROD¹⁴

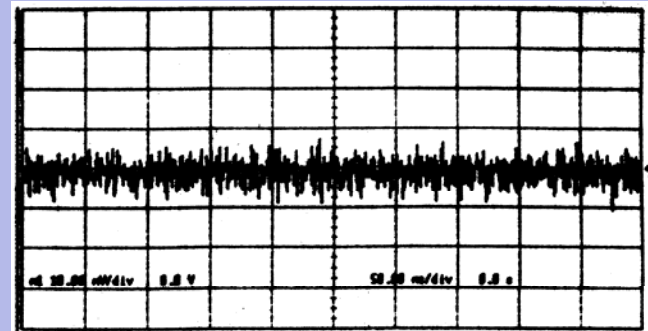
Low Power Beam Intensity (measured using oscilloscope)	20 nW	2 nW	200 pW	20 pW	2 pW
High Power Beam Intensity mW	2	2	0.2	0.2	0.2
Low Power Intensity Measured by Lock-in Amplifier	20.9 nW	2.15 nW	153 ~247 pW	N/A	N/A
r.m.s. Error signal V_{rms} mV	2.01	2.06	2.29	2.03	2.70
r.m.s Phase error rad	0.0286	0.057	0.2	0.16	0.29
Phase-locking time	Longer than observation duration	Longer than observation duration	> 2 hours	> 2 hours	1.5 mins

Results on weak light phase locking for ASTROD (20 pW)



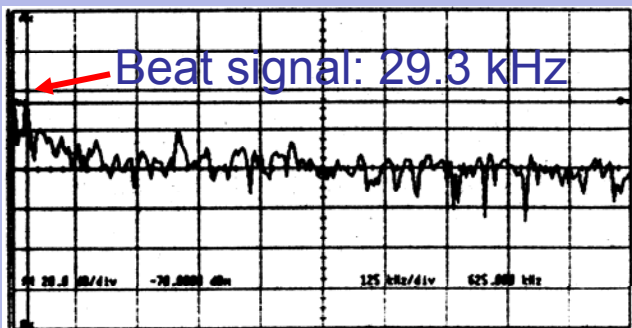
Error signal

X: 20 μ s/div
Y: 10 mV/div

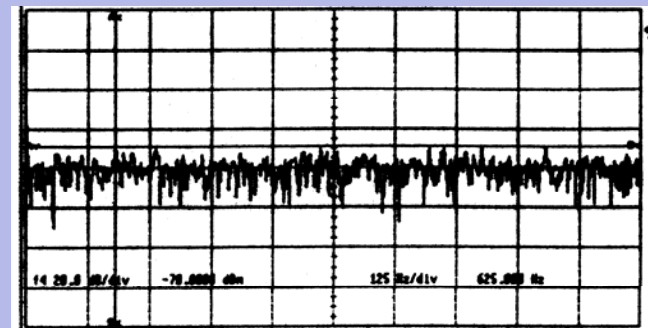


Locked

X: 50 ms/div
Y: 10 mV/div



FFT of the Error signal



FFT of the Locked signal

X: 125 kHz/div
Y: 20 dB/div-70 dBm

Conclusions

- ASTROD is a multi-purpose space mission employing pulse and interferometric ranging to measure relativistic and solar system parameters, and low-frequency gravitational waves.
- A ten-fold improvement in acceleration noise would allow us to reach relativistic parameter uncertainties at the ppb level.
- **Close collaboration among the international scientific community is needed to achieve the scientific objectives and technological challenges required by ASTROD!**

References

- [1] A. Bec-Borsenberger, J. Christensen-Dalsgaard, M. Cruise, A. Di Virgilio, D. Gough, M. Keiser, A. Kosovichev, C. Lämmerzahl, J. Luo, W.-T. Ni, A. Peters, E. Samain, P. H. Scherrer, J.-T. Shy, P. Touboul, K. Tsubono, A.-M. Wu and H.-C. Yeh, *Astrodynamical Space Test of Relativity using Optical Devices ASTROD --- A Proposal Submitted to ESA in Response to Call for Mission Proposals for Two Flexi-Missions F2/F3*, January 31, 2000; and references therein.
- [2] W.-T. Ni ASTROD—an overview., *Int J. Mod. Phys D*. vol. 11 No 7 (2002) 947-962; and references therein.
- [3] W.-T. Ni, “ASTROD and ASTROD I: an overview,” *General Relativity and Gravitation*, Vol. 37, submitted, 2006.
- [4] **Wei-Tou Ni, Henrique Araújo, Gang Bao, Hansjörg Dittus, Tianyi Huang, Sergei Klioner, Sergei Kopeikin, George Krasinsky, Claus Lämmerzahl, Guangyu Li, Hongying Li, Lei Liu, Yu-Xin Nie, Antonio Pulido Patón, Achim Peters, Elena Pitjeva, Albrecht Rüdiger, Etienne Samain, Diana Shaul, Stephan Schiller, Sachie Shiomi, M. H. Soffel, Timothy Sumner, Stephan Theil, Pierre Touboul, Patrick Vrancken, Feng Wang, Haitao Wang, Zhiyi Wei, Andreas Wicht, Xue-Jun Wu, Yan Xia, Yaoheng Xiong, Chongming Xu, Jun Yan, Hsien-Chi Yeh, Yuan-Zhong Zhang, Cheng Zhao, and Ze-Bing Zhou** “ASTROD and ASTROD I: Progress Report” *Journal of Physics: Conference Series* 32 (2006) 154-160. Sixth Edoardo Amaldi Conference on Gravitational Waves
- [5] Ni W-T, Bao Y, Dittus H, Huang T, Lämmerzahl C, Li G, Luo J, Ma Z, Mangin J, Nie Y, Peters A, Rüdiger A, Samain È, Schiller S, Shiomi S, Sumner T, Tang C-J, Tao J, Touboul P, Wang H, Wicht A, Wu X, Xiong Y, Xu C, Yan J, Yao D, Yeh H-C, Zhang S, Zhang Y and Zhou Z 2003 “ASTROD I: Mission Concept and Venus Flybys” *Proc. 5th IAA Int. Conf. On Low-Cost Planetary Missions, ESTEC, Noordwijk, The Netherlands, 24-26 September 2003*, ESA SP-542 79-86; *ibid* 2006 *Acta Astronautica* **58** in press
- [6]. S. Shiomi, and W.-T. Ni. Acceleration disturbances and requirements for ASTROD I. Submitted to *Class. Quantum Grav*, in press.
- [7] Pulido Patón A and Ni W-T 2006 “The low-frequency sensitivity to gravitational waves for ASTROD” *General Relativity and Gravitation* **37** in press; and references therein
- [8]. Ke-Xun Sun et al. Advanced gravitational referente sensor for high precision space interferometer. *Class. Quantum Grav.* 22 (2005) S287-S296.
- [9]. C.C. Speake, S.M. Aston, *Class. Quantum Grav.* 22 (2005) S269-S277)
- [10] F. Acernese et al. *Class. Quantum Grav.* 22 (2005) S279-S285.
- [11] S. Shiomi 2005. “Acceleration disturbances due to local gravity gradients in ASTROD I”, *Journal of Physics: Conference Series* 32 (2006) 186-191. Sixth Edoardo Amaldi Conference on Gravitational Waves
- [12] D. Shaul , T. Sumner, G. Rochester, Coherent Fourier components in the LISA measurement bandwidth from test mass charging: Estimates and suppression, *International Journal of Modern Physics D*, 14, pp51-71.
- [13] Ke-Xun Sun, Brett Allard, Saps Buchman, Scott Williams and Robert L Byer, LED deep UV source for charge management of gravitational reference sensors, *Class.Quantum Grav.* 23(2006) S141-S150.
- [14] **An-Chi Liao, Wei-Tou Ni, Jow-Tsong Shy**, *Int. J. Mod. Phys. D* **11**, 1075 (2002)

Purple Mountain Observatory (Nanjing, China)

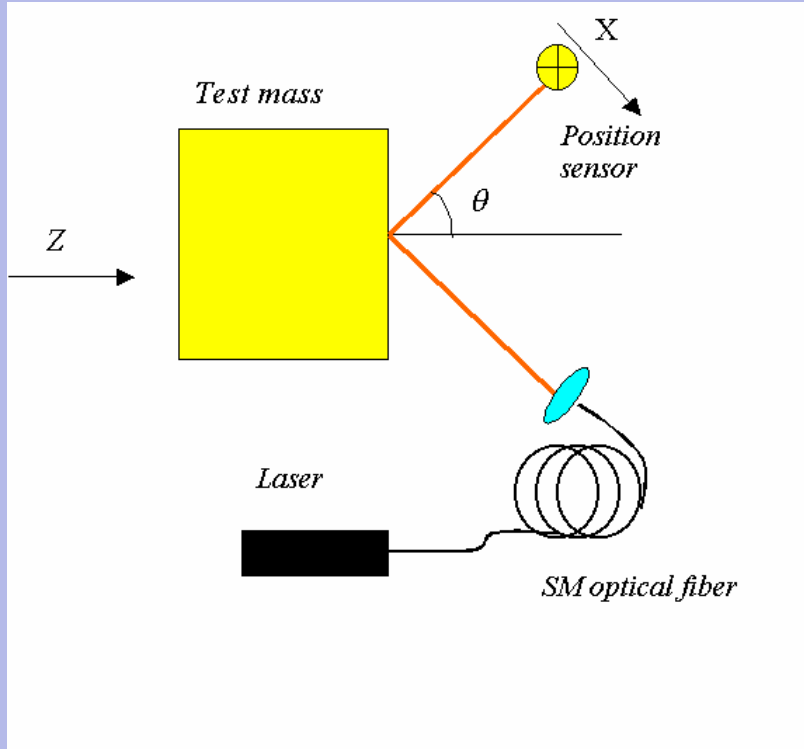


Back-up slides

Acceleration disturbances

- Position dependent (stiffness terms): a) sensor readout noise and b) external environmental disturbances affecting the spacecraft including thruster noise.
- Direct acceleration disturbances: a) environmental disturbances and b) sensor back action disturbances.
- For sensing proof mass-spacecraft relative displacement and control actuation both **capacitive** and/or **optical** sensing will be considered.

Efforts towards optical sensing I

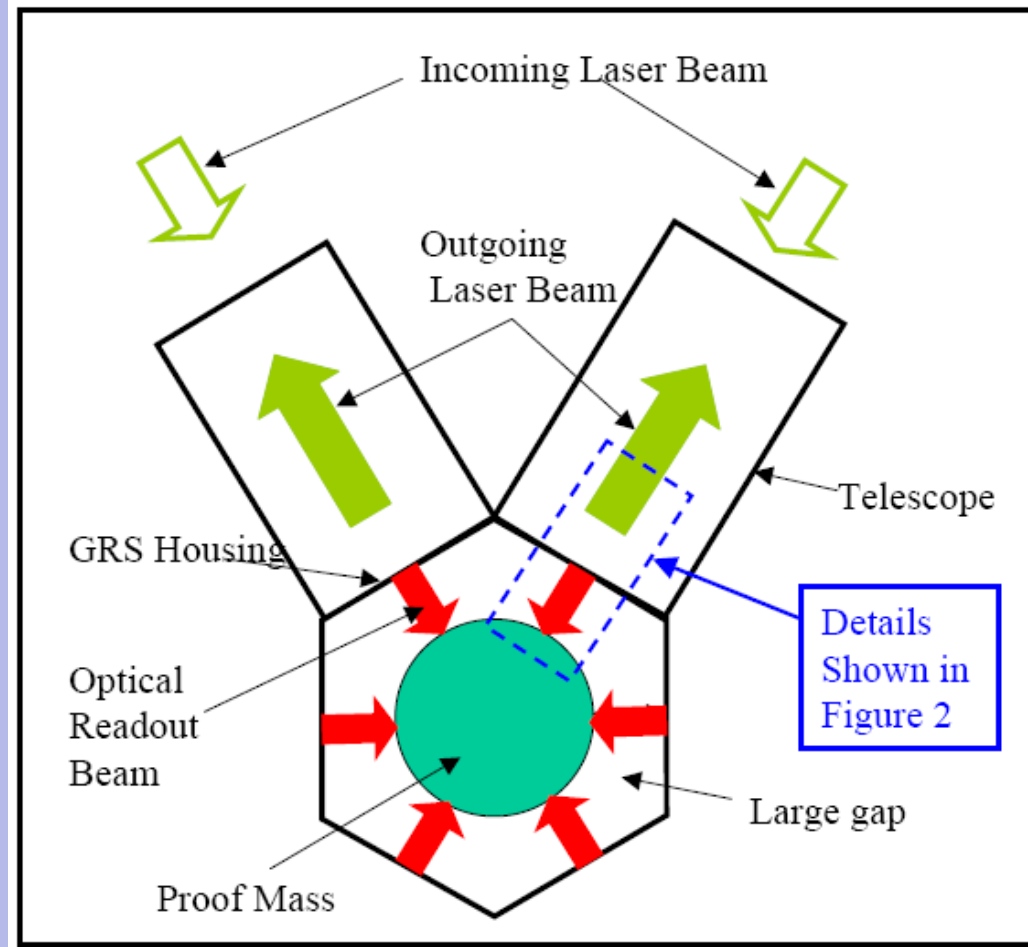


- Relevant noise sources: a) shot noise and b) amplifier current noise ($f^{-1/2}$).
- Back action force disturbance depends on power fluctuations.
- In Acernese et al. [10] they achieve displacement readouts of the order of 10^{-9} m $\text{Hz}^{-1/2}$ down to 1 mHz.

- Optical lever. A test mass displacement induces a transversal beam displacement which is detected by the position sensor.

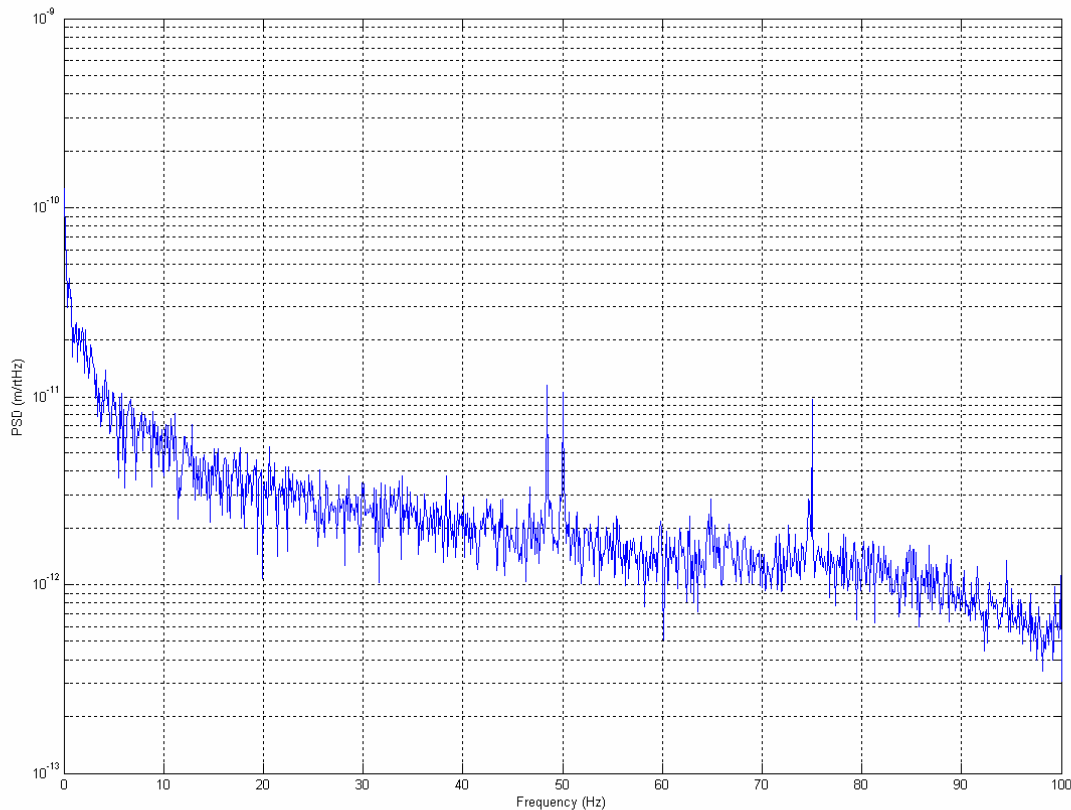
Efforts towards optical sensing II

- Figure on the right side shows a GRS where the test masses are merged into a spherical proof mass [8].
- They consider all-reflective grating beam splitters, minimizing optical path errors due to temperature dependence refractive index. They demonstrate an optical sensing of 30 pmHz^{-12} .

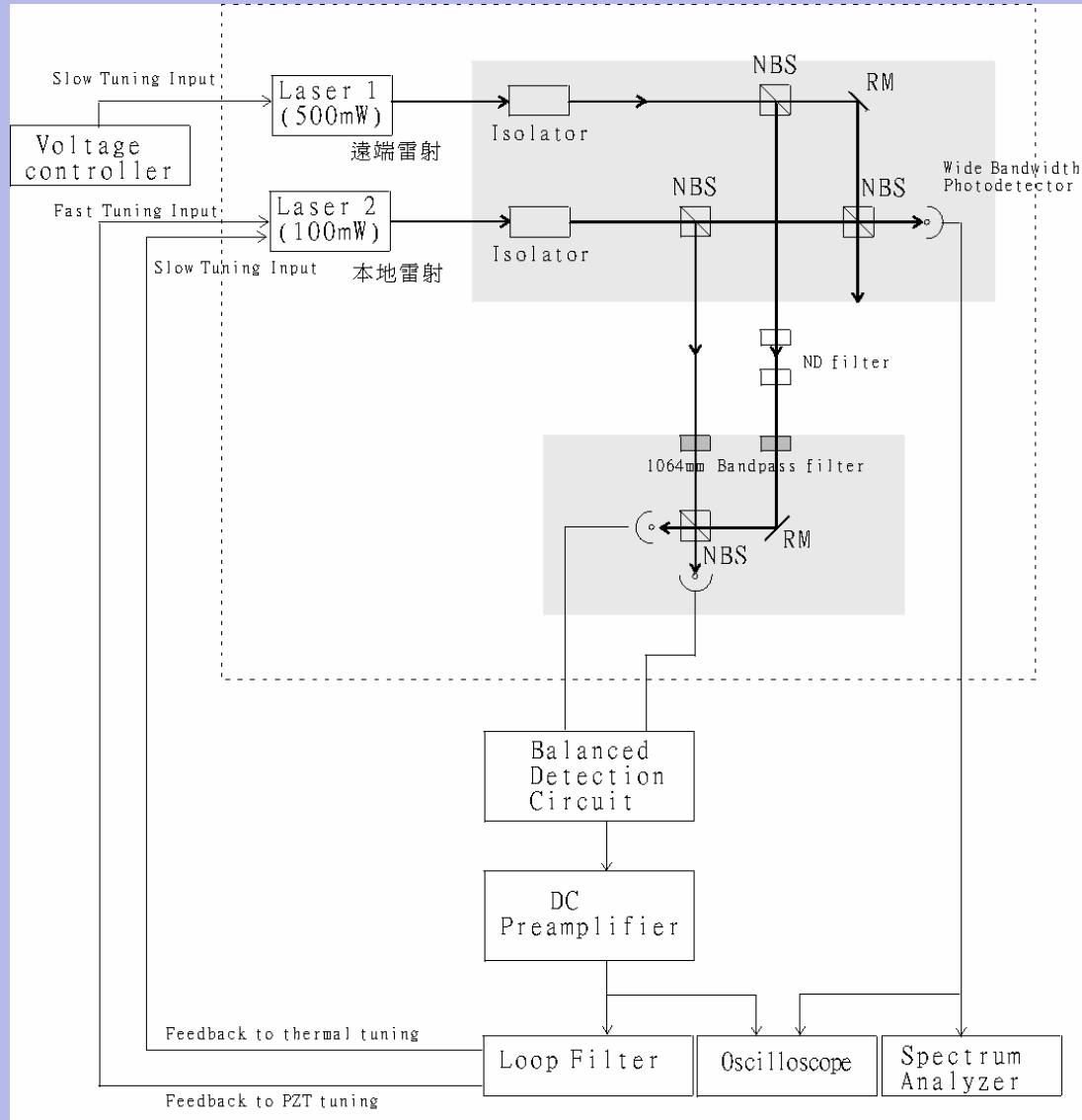


Efforts towards optical sensing III

- In Speake et al. [9] a prototype bench top polarization-based homodyne interferometer based on wavelength modulation technique achieve a shot limited displacement sensitivity of $3\text{pmHz}^{-1/2}$ above 60Hz (using 850 nm VCSEL with 60 nW optical power).



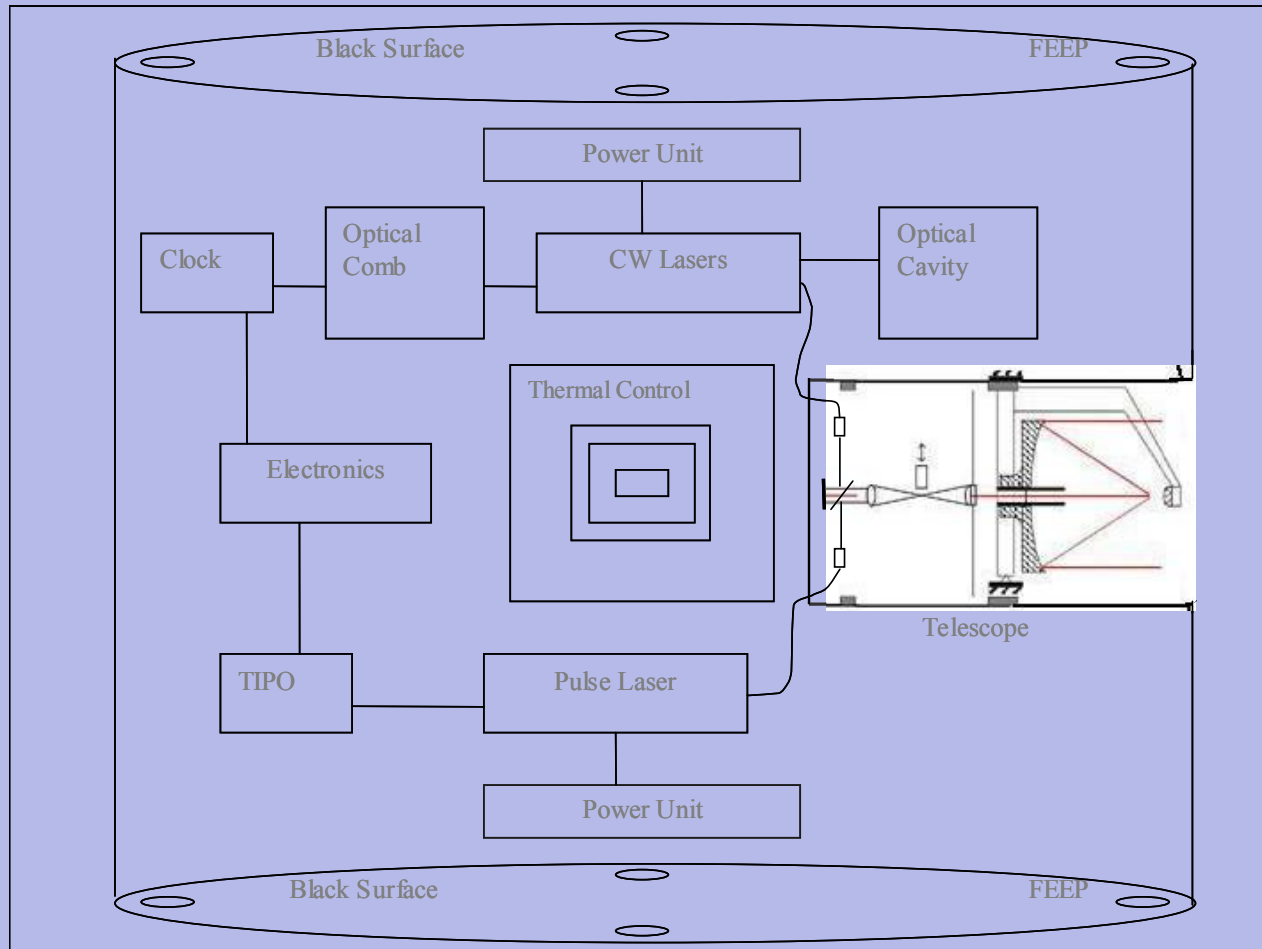
Experimental set-up



ASTROD I spacecraft: general features

1. Cylindrical spacecraft with diameter 2.5 m, 2 m height, and surface covered with solar panels.
2. In orbit, the cylindrical axis is perpendicular to the orbit plane with the telescope pointing toward the ground laser station. The effective area to receive sunlight is about 5 m² and can generate over 500 W of power.
3. The total mass of spacecraft is 300-350 kg. That of payload is 100-120 kg.
4. Science rate is 500 bps. The telemetry rate is 5kbps for about 9 hours in two days.

ASTROD I spacecraft schematic design



ASTROD I science objectives

- Testing relativistic gravity and the fundamental laws of spacetime with three-order-of-magnitude improvement in sensitivity;
- Improving astrodynamics with laser ranging in the solar system, increasing the sensitivity of solar, planetary and asteroid parameter determination by 1-3 orders of magnitude;
- Improving the sensitivity in the $5\mu\text{Hz}$ – 5mHz low frequency gravitational-wave detection by several times (Auxiliary goal).

Proof mass acceleration disturbances

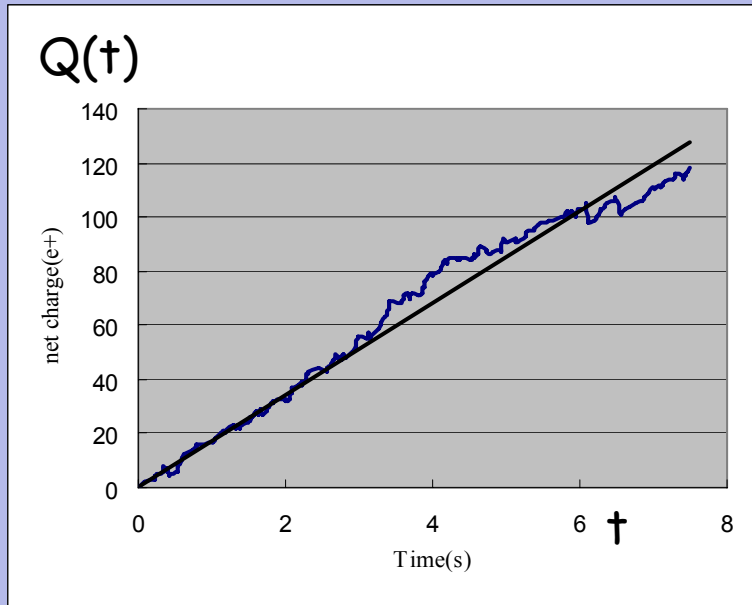
Sources of disturbances	Expressions	Frequency dependence	Noise (units $10^{-16} \text{ms}^{-2}\text{Hz}^{-1/2}$)
Cosmic rays	$f_{CR} = \frac{\sqrt{2mE\lambda}}{m_p}$	1.5×10^{-2}	1.5×10^{-2}
Residual gas	$f_{RG} = \frac{\sqrt{2PA_p}}{m_p} (3k_B T_p m_N)^{1/4}$	$2.9 \left(\frac{P}{3 \times 10^{-6}} \right)^{1/2}$	1.7
Magnetic susceptibility I (χ).	$f_{m1} = \frac{2\chi}{\mu_0 \rho} \frac{1}{\xi_m} \delta B_{SC} \nabla B_{SC}$	$0.72 \left(\frac{\chi}{3 \times 10^{-6}} \right) \frac{1}{\xi_m}$	0.072
Magnetic susceptibility II (χ)	$f_{m2} = \frac{\sqrt{2}\chi}{\mu_0 \rho} \frac{1}{\xi_m} \nabla B_{SC} \delta B_{IP}$	$1.4 \frac{1}{\xi_m} \left(\frac{\chi}{3 \times 10^{-6}} \right) \left(\frac{0.1\text{mHz}}{f} \right)^{2/3}$	0.14
Permanent magnetic moment	$f_{m3} = \frac{1}{\sqrt{2}m_p \xi_m} M_r \nabla(\delta B) $	$5.7 \frac{1}{\xi_m} \left(\frac{ M_r }{1.1 \times 10^{-8}} \right)$	0.57
Lorentz I.	$f_{L1} = \frac{v}{m_p} \frac{1}{\xi_e} q \delta B_{IP}$	$9.1 \times 10^{-2} \left(\frac{\bar{Q}t}{10^{-13}} \right) \left(\frac{100}{\xi_e} \right) \left(\frac{0.1\text{mHz}}{f} \right)^{2/3}$	9.1×10^{-3}
Lorentz II.	$f_{L2} = \frac{v}{m_p} \frac{1}{\xi_e} B_{IP} \delta q$	$1.7 \times 10^{-3} \left(\frac{\bar{Q}}{288} \right)^{1/2} \left(\frac{100}{\xi_e} \right) \left(\frac{0.1\text{mHz}}{f} \right)$	$2 \times 1.7 \times 10^{-3}$
Radiometer effect	$f_{RE} = \frac{A_p P}{2m_p} \frac{1}{\xi_{TS}} \frac{\delta T_{OB}}{T_p}$	$4.7 \left(\frac{P}{3 \times 10^{-6}} \right) \frac{1}{\xi_{TS}}$	1.0×10^{-2}
Out gassing effect	$f_{OG} = 10 f_{RE}$	$47 \left(\frac{P}{3 \times 10^{-6}} \right) \frac{1}{\xi_{TS}}$	1.0×10^{-1}
Thermal radiation pressure	$f_{TR} = \frac{8\sigma}{m_p} \frac{A_p}{c} T_p^3 \frac{\delta T_{OB}}{\xi_{TS}}$	$12 \frac{1}{\xi_{TS}}$	0.08
Gravity Gradient	$f_{GG} = \frac{2GM}{r^2} \alpha \delta T_{SC}$	$0.54 \left(\frac{M}{1\text{kg}} \right) \left(\frac{\delta T_{SC}}{0.004\text{KHz}^{-1/2}} \right)$	0.54
Total proof mass acceleration noise at 0.1 mHz ($\text{ms}^{-2}\text{Hz}^{-1/2}$)			1.9

Back action disturbances (Capacitive sensing)

Source of disturbances	Expressions	Frequency dependence	Noise in units ($10^{-16} \text{ ms}^{-2} \text{ Hz}^{1/2}$)
Quantization	$f_q = \frac{10 F_{x0} }{m_p} \frac{1}{2^N} \frac{1}{\sqrt{12}V_s}$	$6.3 \times 10^{-4} \left(\frac{V_d}{5 \times 10^{-3}} \right) \left(\frac{V_{x0}}{10^{-2}} \right)$	1.3×10^{-5}
Dielectric losses	$f_{DL} = \frac{\sqrt{2}C_x}{m_p d} V_{x0} \delta v_{diel}$	$8 \left(\frac{\delta}{10^{-5}} \right)^{1/2} \left(\frac{V_0}{0.1} \right) \left(\frac{4 \times 10^{-3}}{d} \right) \left(\frac{0.1 \text{mHz}}{f} \right)^{1/2}$	0.25
Voltage	$f_{\delta V_d,1} = \frac{C_x}{m_p d} \frac{C_x}{C} (V_{x0} - V_g) \delta V_d$	$0.145 \left(\frac{V_{0g}}{10^{-2}} \right) \left(\frac{\delta V_d}{10^{-5}} \right) \left(\frac{4 \times 10^{-3}}{d} \right)$	0.145
Charging-Voltage 1	$f_{\delta V_d,2} = \frac{q}{dm_p} \frac{C_x}{C} \delta V_d$	$0.24 \left(\frac{4 \times 10^{-3}}{d} \right) \left(\frac{q}{10^{-13}} \right) \left(\frac{\delta V_d}{10^{-5}} \right)$	2.4×10^{-2}
Charging-Voltage 2	$f_{\delta q,1} = \frac{1}{dm_p} \frac{C_x}{C} V_d \delta q$	$2 \times 7 \left(\frac{4 \times 10^{-3}}{d} \right) \left(\frac{V_d}{5 \times 10^{-3}} \right) \left(\frac{\bar{Q}}{288} \right)^{1/2} \left(\frac{0.1 \text{mHz}}{f} \right)$	0.28
Charging	$f_{\delta q,2} = \frac{q}{m_p d^2} \frac{C_x}{C^2} \Delta d \delta q$	$0.01 \left(\frac{q}{10^{-13}} \right) \left(\frac{\Delta d}{10 \mu\text{m}} \right) \left(\frac{\bar{Q}}{288} \right)^{1/2} \left(\frac{4 \times 10^{-3}}{d} \right)^2 \left(\frac{0.1 \text{mHz}}{f} \right)$	10^{-3}
Total sensor back action disturbance (capacitance)			0.4

Coherent Fourier components

- Arise due to steady **build up of charge** on the test mass



$$Q(t) = \overline{\dot{Q}} t + \delta Q(t)$$

Coherent terms

Coulomb:

$$e_k(t) \equiv \Theta_k t \equiv -\frac{\overline{\dot{Q}} C_x}{m C_T d} V_d t$$

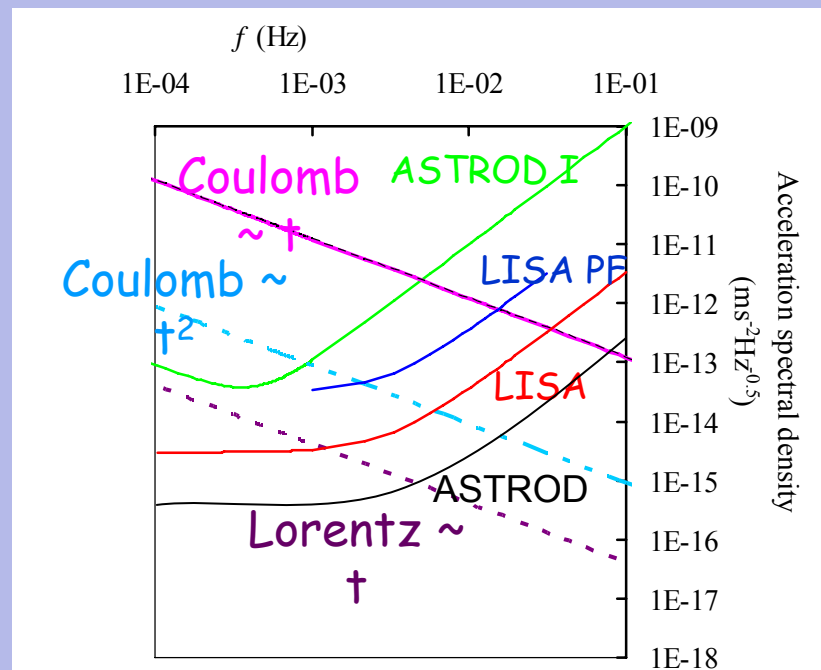
$$f_k(t) \equiv \Xi_k t^2 \equiv \frac{2 \overline{\dot{Q}}^2}{C_T^2 m d^2} t^2 \Delta d$$

Lorentz:

$$l_x(t) \equiv \Phi_x t \equiv \left(\overline{\dot{Q}} v B_{ip} t / m \xi_e \right)$$

Coherent Charging Signals (CHS)

- CHS due to Coulomb forces are due to **geometric** (machining accuracy) and **voltage offsets** (non-uniformity in the sensor surfaces, to minimise work function differences, patch effects, etc) in the capacitive sensor.
- These signal **increases at low frequencies**.
- The magnitude of these signals have been shown to compromise the target acceleration noise sensitivity of LISA (see D. N. A. Shaul [9])
- Ways of dealing and/or suppressing these signals are also discussed in [9].



Discharging schemes

- Accumulation of charge in the test mass induces acceleration disturbances through Lorentz and Coulomb interactions (if employing capacitive sensing).
- Position dependent Coulomb forces also contributes to the coupling between the proof mass and the spacecraft.
- Discharging periodically the proof mass to maintain this signals under the allowable limits, introduce coherent Fourier components as mentioned before.
- These CHS can spoil the sensitivity for a mission as LISA and therefore for ASTROD. Therefore there is a need for looking into continuous discharging schemes to suppress CHS.
- Recently, a deep UV LED as the promising light source for charge management was identified by Ke-Xun Sun et al. (Hansen Experimental Physical Laboratory, Stanford University, CA 94305-4085, USA). This system could have advantages over the more traditional mercury lamp-based system in three key areas: power efficiency, lower weight and flexible functionalities including AC operation out of the science measurement band

Stiffness terms

PM-space craft stiffness	Expressions	Parameter dependence	Units (s ⁻²) 0.1mHz
Image charges	$K_c = \frac{q^2}{d^2 m_p} \frac{C_x}{C^2}$	$1.65 \times 10^{-12} \left(\frac{q}{10^{-13}} \right)^2 \left(\frac{4 \times 10^{-3}}{d} \right)^2$	1.65×10^{-14}
Applied voltage	$K_V = \frac{C_x}{m_p d^2} \left[\left(\frac{C_x}{C} + \frac{1}{4} \right) V_d^2 + \left(\frac{C_g}{C} \right)^2 V_{0g}^2 \right]$	$8.6 \times 10^{-13} \left[10.4 \left(\frac{V_d}{5 \times 10^{-3}} \right)^2 + 2.8 \left(\frac{V_{0g}}{10^{-2}} \right)^2 \right]$	2.4×10^{-12}
$q \times V_{0g}$	$K_{CV} = \left(\frac{2}{m_p d^2} \right) \left(\frac{C_x}{C} \right) \left(\frac{C_g}{C} \right) q V_{0g}$	$2 \times 10^{-12} \left(\frac{4 \times 10^{-3}}{d} \right)^2 \left(\frac{q}{10^{-13}} \right) \left(\frac{V_{0g}}{10^{-2}} \right)$	2×10^{-13}
Patch fields	$K_{PF} = \gamma \frac{C_x}{m_p d^2} \left(\frac{C_x}{C} \right)^2 V_{pe}^2$	$0.3 \times 10^{-9} \left(\frac{4 \times 10^{-3}}{d} \right)^2 \left(\frac{V_{pe}}{0.1} \right)$	3×10^{-10}
Gravity Gradient	$K_{GG} = \frac{2GM}{r^3}$	$3.2 \times 10^{-10} \left(\frac{M_{dis}}{1kg} \right) \left(\frac{0.75}{r} \right)^3$	3.2×10^{-10}
Induced magnetic moment	$K_{m1} = \frac{2\chi}{\rho\mu_0} \left[\nabla B_{SC} ^2 + B_{SC} \nabla^2 B_{SC} \right]$	$5.4 \times 10^{-15} \left(\frac{\chi}{3 \times 10^{-6}} \right)$	5.4×10^{-15}
Magnetic remnant moment	$K_{m2} = \frac{1}{\sqrt{2}m_p} M_r \nabla^2 B_{SC} $	$7.9 \times 10^{-14} \left(\frac{ M_r }{1.1 \times 10^{-8}} \right)$	7.9×10^{-14}
Total stiffness (Capacitance)			4.4×10^{-10}

In the case of employing optical sensing the stiffness will be limited by **gravity gradients**. In a preliminary study for ASTROD I a stiffness value associated to gravity gradients when considering a **cylindrical spacecraft and a parallelepiped proof mass** is about **3.5×10⁻¹⁰ s⁻²** and 5.7×10⁻⁸ s⁻² when the proof mass is enclosed in a box (as in the case of capacitive sensing).

ASTROD GRS parameters

Parameter values used in the acceleration noise estimates.		
Proof Mass		
Mass (kg)		1.75
Density (kgm^{-3})		2×10^4
Cross Section (m^2)		0.050×0.035
Temperature (K)		293
Magnetic Susceptibility: χ		3×10^{-6}
Permanent Magnetic Moment: M_r ($\text{Am}^2\text{Kg}^{-1}$)		2×10^{-8}
Maximum charge build-up:		UV light continuous discharging
Velocity [ms^{-1}]		4×10^4
Electrostatic shielding factor ξ_e		100
Magnetic shielding factor ξ_m		10
Optical bench thermal shielding factor ξ_{TS}		150
Residual gas pressure		10^{-6}
Magnetic fields.		
Local Magnetic field	B_{SC} [T]	8×10^{-7}
Local Magnetic field gradient	∇B_{SC} [Tm^{-1}]	3×10^{-6}
Fluctuation in local magnetic field	δB_{SC} [$\text{THz}^{-1/2}$]	1×10^{-7}
Interplanetary magnetic field	B_{ip} [T]	1.2×10^{-7}
Interplanetary magnetic field gradient	δB_{ip} [$\text{THz}^{-1/2}$]	$4 \times 10^{-7} (0.1\text{mHz}/f)^{2/3}$
Gradient of time-varying magnetic field	$\nabla(\delta B)$ [$\text{Tm}^{-1}\text{Hz}^{-1/2}$]	4×10^{-8}
Capacitive sensing		
Capacitance C_x [pF]		6
Capacitance to ground C_g [pF]		6
Total capacitance C [pF]		36
Gap d [mm]		4
Average voltage across opposite surfaces V_{x0} [V]		0.5
Proof mass bias voltage V_{M0} [V]		0.6
Voltage difference to ground $V_{x0}-V_g=V_{0g}$ [V]		0.01
Voltage difference between opposite faces V_d [V]		10^4
Fluctuation voltage difference δV_d [$\text{VHz}^{-1/2}$]		10^{-5}
Residual dc bias voltage on electrodes V_0 [V]		10^{-2}
Loss angle δ		10^{-6}
Gap asymmetry Δd [μm]		10
Quantization		
Net force on the proof mass: F_{x0} [N]		2.5×10^{-14}
Binary digit: N [bits]		16
Sampling frequency: ν_s [Hz]		100

ASTROD I accelerometer parameters (1)

Table 1. Parameter values used in the acceleration noise estimates

$\nu = 0.1$ mHz	ASTROD I
Proof Mass (PM)	
Mass: m_p [kg]	1.75
Density: ρ [kg m ⁻³]	2×10^4
Cross section: A_p [m ²]	0.050×0.035
Temperature: T_p [K]	293
Fluctuation of temperature difference across PM and housing: δT_d [K Hz ^{-1/2}]	1.0×10^{-5}
Maximum charge build-up: q [C]	10^{-12}
Fluctuation in charge: δq [C Hz ^{-1/2}]	6.1×10^{-15}
Magnetic susceptibility: χ_m	5×10^{-5}
Magnetic remanent moment: $ \vec{M}_r $ [A m ²]	1×10^{-7}
Residual gas pressure: P [Pa]	10^{-5}
Electrostatic shielding factors: ξ_e	10
Magnetic shielding factors: ξ_m	1
Spacecraft (SC)	
Mass: M_{sc} [kg]	350
Velocity: v [m s ⁻¹]	4×10^4
Thruster noise [μ N Hz ^{-1/2}]	10
Area facing the Sun: A_{sc} [m ²]	5
Fluctuation of temperature in SC: δT_{sc} [K Hz ^{-1/2}]	0.2

ASTROD I accelerometer parameters (2)

Capacitive sensing	
Capacitance: C_x [pF]	6
Capacitance to ground: C_g [pF]	6
Total capacitance: C [pF]	$(6C_g \approx) 36$
Gap: d [mm]	2
Asymmetry in gap across opposite sides of PM: Δd [μm]	10
Average voltage across opposite faces: $V_{x_0} (\equiv (V_{x1} + V_{x2})/2)$ [V]	0.1
Proof mass bias voltage: V_{M0} [V]	0.6
Voltage difference between V_{x_0} and voltage to ground: V_{0g} [V]	0.05
Voltage difference between opposing faces: V_d [V]	0.01
Fluctuation of voltage difference across opposite faces: δV_d [V Hz ^{-1/2}]	10^{-4}
Residual dc bias voltage on electrodes: V_0 [V]	0.1
Loss angle: δ	10^{-5}
Magnetic fields	
Local magnetic field: B_{sc} [T]	8×10^{-7}
Local magnetic field gradient: $ \vec{\nabla} B_{sc} $ [T m ⁻¹]	3×10^{-6}
Fluctuation in local magnetic field: $ \delta B_{sc} $ [T Hz ^{-1/2}]	1×10^{-7}
Interplanetary magnetic field: B_{ip} [T]	1.2×10^{-7}
Interplanetary magnetic field gradient: $ \delta B_{ip} $ [T Hz ^{-1/2}]	4×10^{-7}
Gradient of time-varying magnetic field: $ \vec{\nabla}(\delta B) $ [T m ⁻¹ Hz ^{-1/2}]	4×10^{-8}
Cosmic rays	
Impact rate: λ [s ⁻¹]	30
Mass of positron: m [kg]	1.7×10^{-27}
Incident energy: E_d [J]	(200 MeV \Rightarrow) 3.2×10^{-11}
Gravity gradients	
Source mass: M_{dis} [kg]	1 in f_{gg} and 0.03 in a_{gg}
Distance from the source mass: x [m]	0.5 in f_{gg} and 0.05 in a_{gg}
Thermal expansion coefficient: CTE (Aluminium) [K ⁻¹]	2.5×10^{-5}
Patch field	
Multiplicative factor: γ	5
Patch field voltage: V_{pe} [V]	0.1

ASTROD I proof mass acceleration noise and back action

Table 3. The estimated values for the proof-mass acceleration disturbances at the frequency of 0.1 mHz. PM and rss denote proof mass and root-sum-square, respectively. The values are in units of $10^{-15} \text{ m s}^{-2} \text{ Hz}^{-1/2}$. See sections 5 and 6, and tables 1 and 2 for notation.

$[10^{-15} \text{ m s}^{-2} \text{ Hz}^{-1/2}]$		Expressions	ASTROD I
(a) PM environmental acceleration disturbances			
f_{m1}	Magnetic	$\frac{2\chi_m}{\rho\mu_0\xi_m} \vec{\nabla} B_{sc} \delta B_{sc}$	1.2
f_{m2}	Magnetic	$\frac{\sqrt{2}\chi_m}{\rho\mu_0\xi_m} \vec{\nabla} B_{sc} \delta B_{ip}$	3.4
f_{m3}	Magnetic	$\frac{1}{\sqrt{2}m_p} \vec{M}_r \vec{\nabla}(\delta B) $	1.6
f_{L1}	Magnetic	$\frac{v}{\xi_e m_p} \delta q B_{ip}$	0.0017
f_{L2}	Magnetic	$\frac{v}{\xi_e m_p} q \delta B_{ip}$	0.91
f_c	Cosmic rays	$\sqrt{\frac{4mE_d\lambda}{m_p^2}}$	0.0015
f_{rg}	Residual gas	$2\sqrt{\frac{PA}{m_p^2}} (3k_B T_p m_N)^{1/4}$	0.74
f_{re}	Radiometric	$\frac{A_p P}{2m_p} \frac{\delta T_d}{T_p}$	0.17
f_{og}	Outgassing	$10f_{re}$	1.7
f_{tr}	Thermal radiation	$\frac{8}{3} \frac{\sigma A_p}{m_p c} T_p^3 \delta T_d$	0.13
f_{gg}	Gravity gradients	$\frac{2GM_{dist}}{x^2} CTE \cdot \delta T_{sc}$	2.7
$\text{rss}(f_{m1} - f_{gg}) \equiv f_{nep}$			5.2
(b) PM sensor back-action acceleration disturbances			
f_{b1}	$\delta V_d \times V_0 g$	$\frac{C_x}{m_p d} \frac{C_g}{C} V_0 g \delta V_d$	1.4
f_{b2}	$\delta V_d \times q$	$\frac{1}{m_p d} \frac{C_x}{C} q \delta V_d$	4.8
f_{b3}	$\delta q \times V_d$	$\frac{1}{m_p d} \frac{C_x}{C} V_d \delta q$	2.9
f_{b4}	$\delta q \times q$	$\frac{1}{m_p d} \frac{C_x}{C^2} \frac{\Delta d}{d} q \delta q$	0.040
f_{ba}	Readout electronics	(see table 1 of [37])	1.8
f_{pe}	Patch fields	$\frac{1}{m_p d} \frac{C_x}{C} V_{pe} \delta q$	29
f_{dl}	Dielectric losses	$\sqrt{2} \frac{C_x}{m_p d} V_0 \delta v_{diel}$	1.6
$\text{rss}(f_{b1} - f_{dl}) \equiv f_{nbp}$			30
$\text{rss}(f_{m1} - f_{dl}) \equiv f_{np}$			30

ASTROD I stiffness terms

Table 4. The proof-mass stiffness in units of 10^{-9} s^{-2} (see sections 6 and 7, and tables 1 and 2 for notation.)

[10^{-9} s^{-2}]		Expressions	ASTROD I
K_{gg}	Gravity gradients	$2 \frac{GM_{d12}}{r^3}$	32
K_{s1}	Image charges	$\frac{1}{m_p C d^2} \left(\frac{C_g}{C} \right) q^2$	0.66
K_{s2}	$q \times V_{0g}$	$\left(\frac{2}{m_p d^2} \right) \left(\frac{C_g}{C} \right) \left(\frac{C_g}{C} \right) q V_{0g}$	0.40
K_{s3}	Applied voltages	$\frac{C_g}{m_p d^2} \left\{ \left(\frac{C_g}{C} + \frac{1}{4} \right) V_d^2 + \left(\frac{C_g}{C} \right)^2 V_{0g}^2 \right\}$	0.095
K_{s4}	Bias voltage	$\frac{C_g}{m_p d^2} V_{M0}^2$	3.1×10^2
K_{s5}	Patch fields	$\gamma \left(\frac{C_g}{m_p d^2} \right) \left(\frac{C_g}{C} \right)^2 V_{pe}^2$	1.2
K_{m1}	Induced magnetic moments	$\frac{2\chi_m}{\rho\mu_0} \left\{ \vec{\nabla} B_{sc} ^2 + B_{sc} \vec{\nabla}^2 B_{sc} \right\}$	9.0×10^{-5}
K_{m2}	Magnetic remanent moments	$\frac{1}{\sqrt{2}m_p} \vec{M}_r \vec{\nabla}^2 B_{sc} $	6.9×10^{-4}
rss($K_{gg} - K_{m2}$) $\equiv K$			3.1×10^2

ASTROD I requirements compared to LISA

Table 5. Relaxed parameter values in comparison with LISA

$\nu = 0.1$ mHz	ASTROD I	LISA
Maximum charge build-up: q [C]	10^{-12}	10^{-13}
Magnetic susceptibility: χ_m	5×10^{-5}	3×10^{-6}
Magnetic remanent moment: $ \vec{M}_r $ [A m ²]	1×10^{-7}	2×10^{-8}
Residual gas pressure: P [Pa]	10^{-5}	3×10^{-6}
Electrostatic shielding factors: ξ_e	10	100
Thruster noise [μ N Hz ^{-1/2}]	10	a few
Fluctuation of temperature in SC: δT_{sc} [K Hz ^{-1/2}]	0.2	0.004
Voltage difference between average voltage across opposite faces and voltage to ground: V_{0g} [V]	0.05	0.01
Voltage difference between opposing faces: V_d [V]	0.01	0.005
Fluctuation of voltage difference across opposite faces: δV_d [V Hz ^{-1/2}]	10^{-4}	10^{-5}
Residual dc bias voltage on electrodes: V_0 [V]	0.1	0.01

Relativistic parameter uncertainties for ASTROD I

- Assuming 10 ps timing accuracy and 10^{-13} $\text{ms}^{-2}\text{Hz}^{-1/2}$ ($f = 0.1$ mHz), a simulation for 400 days (350-750 days after launch) we obtain uncertainties for γ , β and J_2 about 10^{-7} , 10^{-7} and 3.8×10^{-9} .